Electronic Supplementary Information

Thermally-induced Hysteretic Valence Tautomeric Conversions in Solid State via Two-step Labile Electron Transfers in Manganese-Nitronyl Nitroxide 2D-Frameworks

Constance Lecourt,[a] Yuuta Izumi,[b] Lhoussain Khrouz,[c] François Toche,[a] Rodica Chiriac,[a] Nicolas Bélanger-Desmarais,[d] Christian Reber,[d] Oscar Fabelo,[e] Katsuya Inoue,[b] Cédric Desroches,[a] and Dominique Luneau[a*]

a)   Laboratoire des Multimatériaux et Interfaces, UMR CNRS 5615, Univ Lyon, Université Claude Bernard Lyon 1, F-69622 Villeurbanne, France.

E-mail: dominique.luneau@univ-lyon1.fr

b) Department of Chemistry, Graduate School of Science and Chirality Research Center (CResCent), Hiroshima University, 1-3-1, Kagamiyama, Higashi Hiroshima, Hiroshima, 739-8526, Japan

c) Univ Lyon, ENS de Lyon, CNRS UMR 5182, Université Claude Bernard Lyon 1, Laboratoire de Chimie, F69342, Lyon, France

 d) Département de chimie, Université de Montréal, Montréal, Québec, H3C 3J7, Canada.

e) Institut Laue-Langevin, 71 avenue des Martyrs, 38042 Grenoble Cedex 9, France

Materials: 2,3-dihydroxylamino-2,3-dimethylbutane was synthesized following a reported procedure.[1] 2-(2-imidazolyl)-4,4,5,5-tetramethyl-4,5-dihydro-1H-imidazolyl-3-oxide-1-oxy (NITImH) was synthesised from condensation of 2,3-dihydroxylamino-2,3-dimethylbutane with 1H-Imidazole-2-carbaldehyde as previously reported.[2] All other chemicals and solvents were purchased as analytical grade and were used without further purification.

Synthesis of $\{[Mn_2(NITIm)_3]BF_4\}_n$ (2): To 10 mL of a methanol solution of NITImH (100 mg, 0.448 mmol) were added a 10 mL of a methanol solution of $Mn(CH_3COOH)_2.4H_2O$ (73.2 mg, 0.299 mmol). The resulting green-blue solution was then put in the bottom of a test tube and on the top of this solution was added 20 mL of a methanol solution of $NaBF_4$ (18 mg, 0.165 mmol). The tetrafluoroborate solution diffused slowly toward the second solution. A crystalline dark green powder was isolated by filtration after 5 days and was washed with cold methanol. Yield: 35.6 mg, 63 %. Elemental analysis and IR spectrum agree with solvent free compound **2**. Elemental analysis (%): Mn, 11.78; C, 41.16; H, 4.97; N, 19.32; Calculated for $C_{30}H_{42}BF_4Mn_2N_{12}O_6$ (%): Mn, 12.73; H, 41.73; H, 4.90; N, 19.47 ; IR spectrum (v/cm^{-1}) at 293(2) K (**2$_{HT}$**): 2994w, 1568w, 1446s, 1418w, 1394w, 1346s, 1320s, 1214w, 1184w, 1154m, 1142m, 1110w, 1048s, 972w, 950m, 872m, 830w, 794m, 758w, 726w, 652w, 612w.

Raman spectrum (v/cm^{-1}) at 293(2) K (**2$_{HT}$**): 1116w, 1195w, 1458w, 1574s.

Synthesis of $\{[Mn_2(NITIm)_3]PF_6\}_n$ (3): In a beaker, 100 mg of NITImH (0.448 mmol) and 73.2 mg of $Mn(CH_3COOH)_2.4H_2O$ (0.299 mmol) were dissolved in 5 mL of methanol. To this solution was added a 5 mL methanol solution of NBu_4PF_6 (50 mg, 0.129 mmol). The resulting blue-green solution was heated at 50 °C during 10 min and then covered. A crystalline dark green powder was isolated by filtration after 5 days and was washed with cold methanol. Yield: 93 mg, 71%. Elemental analysis and IR spectrum agree with solvent free compound **3**. Elemental analysis (%): Mn, 12.41; C, 38.92; H, 4.66; N, 18.14; Calculated for $C_{30}H_{42}Mn_2N_{12}O_6PF_6$ (%): Mn, 11.92, C, 39.10; H, 4.59; N, 18.24 ; IR spectrum (v/cm^{-1}) at 293(2) K (**3$_{LT}$**): 2992w, 2934w, 1570w, 1450m, 1396w, 1348m, 1322m, 1212w, 1154m, 1140m, 1020w, 954w, 874m, 850s, 794m, 726w, 654w, 612w

Raman spectrum (v/cm^{-1}) at 293(2) K (**3$_{LT}$**): 1116w, 1184w, 1453w, 1574s, 1617m

Single-crystal X-ray diffraction of $\{[Mn_2(NITIm)_3]BF_4\}_n$ (2): A dark blue plate-like specimen of approximate dimensions 0.408 mm x 0.290 mm x 0.032 mm was used for the X-ray crystallographic analysis on a Bruker Smart APEX2 at the Natural Science Center for Basic Research and Development (N-BARD), Hiroshima University. Data collection was carried out at 293(2) K, 252(2) K and 173(2) K with a rotating anode providing X-rays with a wavelength of $\lambda = 0.71073$ Å (Mo-Kα radiation with multi-layered confocal mirror). The data reduction was performed with the Bruker SAINT software package.[3] Data were corrected for absorption effects using the Multi-Scan method (SADABS).[4] SHELXT was used to solve the crystal structures. However, to allow for better comparison with isostructural compounds **1** and **3,** the atom positions of the $[Mn^{II}_2(NITIm)_3]^+$ moiety were taken from the crystal structure of **1** at 300 K.[2, 5] They were first used successfully in the refinement of structure of **2** at 293 K while the BF_4^- anion was found from Fourier difference. Then the resulting positions were in turn used for the refinement at 252 K. The same process was further done for the 173 K data set but in that case the refinement using the atom positions as at 293 K and 252 K required the non-conventional cell ($\beta < 90°$). All refinements were done by full-matrix least-square methods on F^2 with the 2018 version of SHELXL program[6] using the WinGX[7] and OLEX2[8, 9] platforms. All non-hydrogen atoms were refined with anisotropic displacement parameters. Hydrogen atoms belonging to carbon atoms were placed geometrically in their idealized positions and refined using a riding model. The crystal structure parameters and refinement details are summarized in Table 1 and Table S1. Selected bond lengths and bond angles are collected in Table **2**. CCDC numbers: 2002542 (173K), 2002544 (252K) and 2002545 (293K).

X-ray Single-crystal diffraction of $\{[Mn_2(NITIm)_3]PF_6\}_n$ (3): A metallic dark black plate-like specimen of approximate dimensions 0.05 mm x 0.03 mm x 0.02 mm was used for the X-ray crystallographic data collection on the dual-source D8 Venture equipped with a Photon III detector operated at 296(2) K at Institut Laue Langevin in Grenoble. The Copper μ–source was used, providing X-rays with a wavelength of $\lambda = 1.54178$ Å. The data reduction was performed with the Bruker SAINT software package[3] using a narrow-frame algorithm. The integration of the data using a monoclinic unit cell, $a = 10.850(2)$ Å, $b = 17.085(4)$ Å, $c = 11.085(3)$ Å, $\beta = 94.362(16)°$ and a volume of 2049.0(8) Å^3, yielded a total of 18850 reflections to a maximum θ angle of 68.646° (0.83

Å resolution), of which 6880 were independent (completeness = 96.4%, R_{int} = 13.65%, R_{sig} = 11.76%) and 3859 (56.01%) were greater than $2\sigma(F^2)$.

The structure could be solved and refined using the Bruker SHELXTL Software Package,[6] using the space group $P2_1$, with Z = 2 for the formula unit $\{[Mn^{III}_2(NITIm)(NITRed)_2]PF_6\}_n$ ($C_{30}H_{42}F_6Mn_2N_{12}O_6P$) and considering an inversion twin. However, to allow for better comparison with crystal structures of **1** and **2,** the atom positions with labels of the $[Mn^{III}_2(NITIm)(NITRed)_2]^+$ moiety taken from crystal structure of **2** at 173 K were preferred to be used in refinement while PF_6^- anions were found from Fourier difference maps. The final full-matrix least-squares refinement on F^2 with 515 variables converged at R_1 = 12.27%, for and w_{R2} = 29.36% for $2\sigma(F^2)$ data. The goodness-of-fit was 1.074. All non-hydrogen atoms were refined anisotropically. A significant increase in the anisotropic displacement parameters of the PF_6^- counter-anions was observed in comparison with the $[Mn_2(NITIm)_3]^+$ cationic layers. Finally, it deserves to be noted that some weak reflections of the form (h, k, l±0.5) can be indexed, corresponding to a doubling along the *c*-axis and therefore a super-cell can be described which is in agreement with the X-powder diffraction. All our attempts to refine a structural model using this super-cell approach provided results with worse statistics, due to the low intensity of these super-structure reflections. The crystal structure parameters and refinement details are summarized in Table 1 and Table S2. Selected bond lengths and bond angles are collected in Table **2**. CCDC number: 2002547

X-ray Powder diffraction: X-ray powder diffractograms were collected at room temperature on a PANalytical XpertPro MRD diffractometer with a Cu source centered at Kα1 (λ= 1.5406 Å) working at 40 kV/30 mA with θ/θ configuration. Compound powder samples were deposited on a silicon substrate and X-ray data were collecting during thirteen hours.

Magnetic measurements: Magnetic susceptibility data (2-300 K) were collected on powder samples using a SQUID magnetometer (Quantum Design model MPMS-XL) in a 0.1 T applied magnetic field. A magnetization isotherm was collected in the 0-5 T range. All data were corrected for the contribution of the sample holder and diamagnetism of the samples estimated from Pascal's constants.[10, 11]

Electron paramagnetic resonance: EPR assays were carried out using a Bruker EMX spectrometer operating at X-band with double cavity. The instrument settings were as follows: 100 kHz modulation frequency, 0.7-6.9 mW microwave power, 5 G modulation

amplitude, 20.48 ms time constant and one scan of acquisition. Temperature ranges used were 100-350 K and 8-65 K.

Differential Scanning Calorimetry: DSC measurements have been done with the DSC 1 from Mettler Toledo in the temperature range 203-313 K for **2** and 300-400 K for **3**. The heating and cooling rates for all DSC steps were fixed at 5 K.min^{-1} and pure nitrogen was used as reactive gas. The calibration of the DSC was done in the selected temperature range by using the melting enthalpies and temperatures of mercury and indium. The powder sample was analyzed by using a mass of about 3.5 mg into a 40 µL aluminum pan with a pierced lid.

Temperature-modulated DSC: For this method, heating was done in the same temperature range as for regular DSC but the scan rate was 2 K.min^{-1} with an amplitude and a period of the temperature modulation of 0.30 K and 1 min respectively. The Fourier transform analysis was used to measure the amplitude of the response to the temperature modulation. The intention was to check if the VT conversion was dependent on the latent heat (i.e. first order transition) and/or sensible heat (second order transition).

Raman spectroscopy: Raman spectra were measured using a Renishaw InVia spectrometer coupled to an imaging microscope (Leica) and argon ion or diode lasers. The excitation wavelength used was 514 nm. Spectra at variable temperature were measured using a nitrogen gas-flow microcryostat system (Linkam).

Table S1. Crystal data and structure refinement parameters for $\{[Mn_2(NITIm)_3]BF_4\}_n$ (**2**) at 293 K (**2_HT**), 252 K (**2_INT**) and 173 K (**2_LT**).

Formula		$C_{30}H_{42}BF_4Mn_2N_{12}O_6$	
M (g/mol)		863.44	
Shape		plate	
Crystal size (mm)		0.408 x 0.290 x 0.032	
λ (Kα/Mo) (Å)		0.71073	
Crystal system		Monoclinic	
Space group		$P2_1$	
Temperature (K)	**293(2)**	**252(2)**	**173(2)**
CCDC number	2002545	2002544	2002542
a (Å)	10.308(3)	10.532(2)	10.608(9)
b (Å)	17.943(5)	17.537(4)	17.057(15)
c (Å)	11.085(3)	10.786(2)	10.701(9)
β (°)	94.077(3)	93.607(2)	89.585(11)[a]
V (Å^3)	2045.1(10)	1988.2(7)	1936(3)
Z	2	2	2
ρ (g/cm^3)	1.402	1.442	1.481
μ (mm^{-1})	0.690	0.710	0.729
F (000)	890	890	890
θ (°) range for data collection (°)	1.981 to 23.644	1.892 to 29.153	1.903 to 29.376
Limiting indices		-14<=h<=14; -23<=k<=23 ; -14<=l<=14	
Num. Refl. collected / unique	3059 / 3059	23036 / 9685	22233 / 9567
Rint	0.0771	0.0397	0.0917
Completeness (%) to θ° max	95.7	99.9	99.9
Refinement method		Full-matrix least-squares on F^2	
Data / restraints / parameters	3059 / 1 / 508	9685 / 1 / 508	9567 / 1 / 508
GOF (S)	0.866	1.014	0.954
R1[b] / I > 2σ(I)	0.0582,	0.0526,	0.0557,
wR2[c] / I > 2σ(I)	0.1252	0.1233	0.1297
R1[b] (all data)	0.0791	0.0826	0.0858
wR2[c] (all data)	0.1302	0.1386	0.1443
Flack Parameter F	0.05(4)	0.013(10)	0.033(17)
Extinction coefficient	n/a	n/a	n/a
$\Delta\rho_{min}/\Delta\rho_{max}$ (e$^-$/Å^3)	0.666 and -0.652	1.066 and -0.334	1.271d -0.687

[a] The non-conventional crystal cell with β = 89.585(11)° corresponds to the real evolution of crystal parameters from 293 K to 173 K with atomic positions kept as (x, y, z) as at 293K and 252K. For the conventional crystal cell β = 90.415(11)° atomic position have to be change as (x, -y, -z) from the one at 293 K and 252 K. [b] $R_1 = \Sigma||Fo|-|Fc||/\Sigma|Fo|$, [c] $wR_2 = [\Sigma(w(Fo^2-Fc^2)^2)/ \Sigma(\omega(Fo^2)^2)]^{1/2}$ avec $\omega = 1/[(\sigma^2 Fo^2)+(aP)^2+bP]$ et $P = (max(Fo^2)+2Fc^2)/3$

Table S2. Crystal data and structure refinement parameters for $\{[Mn^{III}_2(NITIm)(NITIm)_2]PF_6\}_n$ (**3$_{LT}$**) at 296 K.

Formula	$C_{30}H_{42}F_6Mn_2N_{12}O_6P$
CCDC number	2002547
M (g/mol)	921.61
Shape	Plate
Crystal size (mm)	0.050 x 0.030 x 0.010
λ (Kα/Cu) (Å)	1.54178
Crystal system	Monoclinic
Space group	$P2_1$
Temperature (K)	296(2)
a (Å)	10.850(2)
b (Å)	17.085(4)
c (Å)	11.085(3)
β (°)	94.362(16)
V (Å^3)	2049.0(8)
Z	2
ρ (g/cm^3)	1.432
μ (mm^{-1})	6.022
F (000)	910
θ (°) range for data collection (°)	3.999 to 68.646
Limiting indices	-11<=h<=12 ;-20<=k<=20 ; -13<=l<=13
Num. Refl. collected / unique	18850 / 6880
Rint	0.1176
Completeness (%) to θ° max	96.4
Refinement method	Full-matrix least-squares on F^2
Data / restraints / parameters	6880 / 1 / 515
GOF (S)	1.074
R1^a / I > 2σ(I)	0.1228,
wR2^b / I > 2σ(I)	0.2937
R1^a (all data)	0.1846,
wR2^b (all data)	0.3399
Flack Parameter F	NA (refined as inversion twin)
Extinction coefficient	n/a
$\Delta\rho_{min}/\Delta\rho_{max}$ (e$^-$/Å^3)	2.443 and -0.533

(a) $R_1 = \Sigma||Fo|-|Fc||/\Sigma|Fo|$, (b) $wR_2 = [\Sigma(w(Fo^2-Fc^2)^2)/\Sigma(\omega(Fo^2)^2)]^{1/2}$ avec $\omega = 1/[(\sigma^2Fo^2)+(aP)^2+bP]$ et $P = (max(Fo^2)+2Fc^2)/3$

Table S3. Crystal parameters for compound **1**, **2** and **3**.

| Compound	1^5				2				3
Formula	$C_{30}H_{42}Mn_2N_{12}O_6ClO4$				$C_{30}H_{42}Mn_2N_{12}O_6BF_4$				$C_{30}H_{42}Mn_2N_{12}O_6PF_6$
M (g/mol)	876.09				863.44				921.61
Crystal system	Monoclinic				Monoclinic				Monoclinic
Space group	$P2_1$				$P2_1$				$P2_1$
T(K)	313(2)	233(2)	193(2)	Δ1 (%)	293(2)	252(2)	173(2)	Δ2 (%)	296
a (Å)	10.325(1)	10.597(4)	10.688(3)	+ 3.5	10.308(3)	10.532(2)	10.608(9)	+2.9	10.850(2)**
b (Å)	17.870(1)	17.037(7)	17.165(5)	- 3.9	17.943(5)	17.537(4)	17.057(15)	-4.9	17.085(4)
c (Å)	11.063(1)	10.657(5)	10.761(4)	- 2.7	11.085(3)	10.786(2)	10.701(9)	-3.5	11.085(3)
β (°)	93.430(4)	90.623(8)	90.648(6)	- 3.0	94.077(3)	93.607(2)	89.585(11)*	-4.8	94.362(16)
V (Å^3)	2037.5(3)	1924.0(1)	1974.1(1)	- 3.1	2045.1(10)	1988.2(7)	1936(3)	-5.3	2049.0(8)

*Non-conventional crystal cell respective of the evolution of crystal parameters from 293K to 173K with atomic positions (*x*, *y*, *z*) from 293 K and 252 K. ** For comparison *a* and *c* axis are permuted with respect to **1** and **2**. Δ1: Variation on crystal parameters from 313 K to 193 K for **1**. Δ2: Variation on crystal parameters from 293 K to 173 K for **2**.

Table S4. BVS calculations for the oxidation state of Mn1 and Mn2 of compound **2** at each temperature.
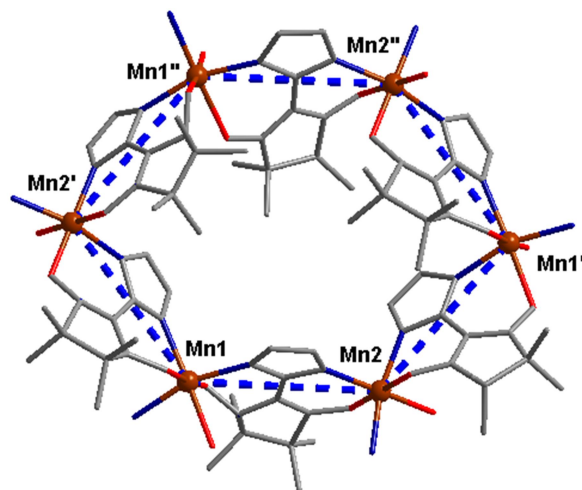
Compound	2			3
T (K)	293	252	173	296
Mn1 (+II/+III)	**2.30**/2.12	**2.36**/2.18	3.35/**3.08**	3.36/**3.10**
Mn2 (+II/+III)	**2.30**/2.12	3.28/**3.03**	3.44/**3.17**	3.44/**3.17**

Table S5. Atomic deviation (Å) from selected mean planes.

radical nitronyl nitroxide   reduced form
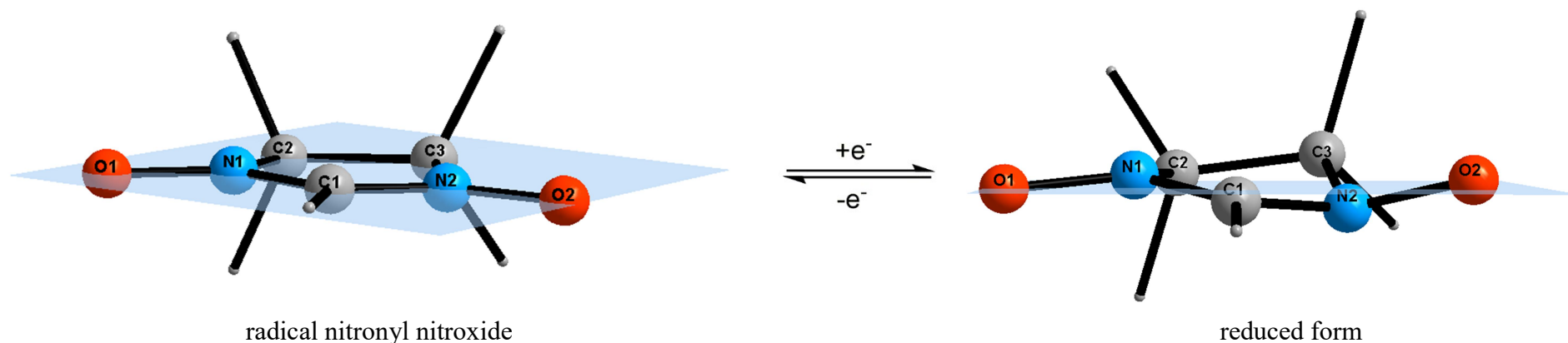
Radical	A				B				C			
Compound	2			3	2			3	2			3
T (K)	293	252	173	296	296	252	173	296	293	252	173	296
Mean plane	O1A-N1A-C1A-N2A-O2A				O1B-N1B-C1B-N2B-O2B				O1C-N1C-C1C-N2C-O2C			
O1	0.004	0.007	0.072	0.070	0.036	0.022	0.009	0.011	0.029	0.051	0.191	0.232
N1	0.019	0.141	0172	0.181	0.024	0.025	0.012	0.006	0.018	0.030	0.182	0.181
C1	0.006	0.099	0.006	0.029	0.037	0.014	0.004	0.012	0.026	0.048	0.192	0.248
N2	0.024	0.172	0.183	0.177	0.007	0.014	0.009	0.002	0.010	0.019	0.148	0.115
O2	0.016	0.137	0.091	0.095	0.030	0.003	0.001	0.009	0.025	0.046	0.035	0.082
Mean plane	O1A-C1A-C2A				O1B-C1B-C2B				O1C-C1C-C2C			
N1	0.007	0.137	0.266	0.230	0.036	0.034	0.016	0.012	0.035	0.016	0.351	0.377
Mean plane	O2A-C1A-C3A				O2B-C1B-C3B				O2C-C1CA-C3C			
N2	0.024	0.301	0.229	0.282	0.013	0.035	0.034	0.012	0.022	0.035	0.142	0.086

Table S6. Inter-atomic Mn---Mn distances (Å) in compounds **1**, **2** and **3** in an alveoli of the honeycomb-like structure at different temperature.

Compound	1^5			2			3
T(K)	*300*	*233*	*193*	*293*	*252*	*173*	*296*
Mn1-Mn2	6.2103(48)	6.0186(90)	6.0697(78)	6.2444(23)	6.1082(14)	6.0433(44)	5.9837(40)
Mn1-Mn2'	6.2809(51)	5.9427(90)	5.9951(78)	6.2454(23)	6.1404(14	5.9560(43)	6.0964(38)
Mn1-Mn1'	11.0192(49)	10.9133(87)	11.003(79)	11.3830(30)	11.0898(20)	10.9614(69)	10.850(5)
Mn1-Mn1"	11.3081(50)	9.4010(83)	9.4393(77)	9.9752(33)	9.7588(21)	9.4127(70)	9.4298(42)
Mn1-Mn2"	11.4787(49)	11.3523(86)	11.4302(80)	11.9565(41)	11.7998(28)	11.3682(98)	11.1529(41)
Mn2-Mn1'	6.2127(48)	6.0283(78)	6.0838(76)	6.3294(30)	6.1211(16)	6.0532(50)	6.0802(40)
Mn2-Mn2"	11.2646(50)	9.4373(83)	9.5174(77)	11.3407(32	9.7295(21)	9.4497(70)	9.4846(38)
Mn2-Mn1"	11.8948(52)	10.9589(94)	11.0708(81)	11.5276(31)	11.2099(19)	10.9838(72)	11.2796(44)
Mn1'-Mn2'	13.7889(49)	13.4062(102)	13.5301(86)	13.8922(36)	13.4888(24)	13.4781(95)	13.6159(44)
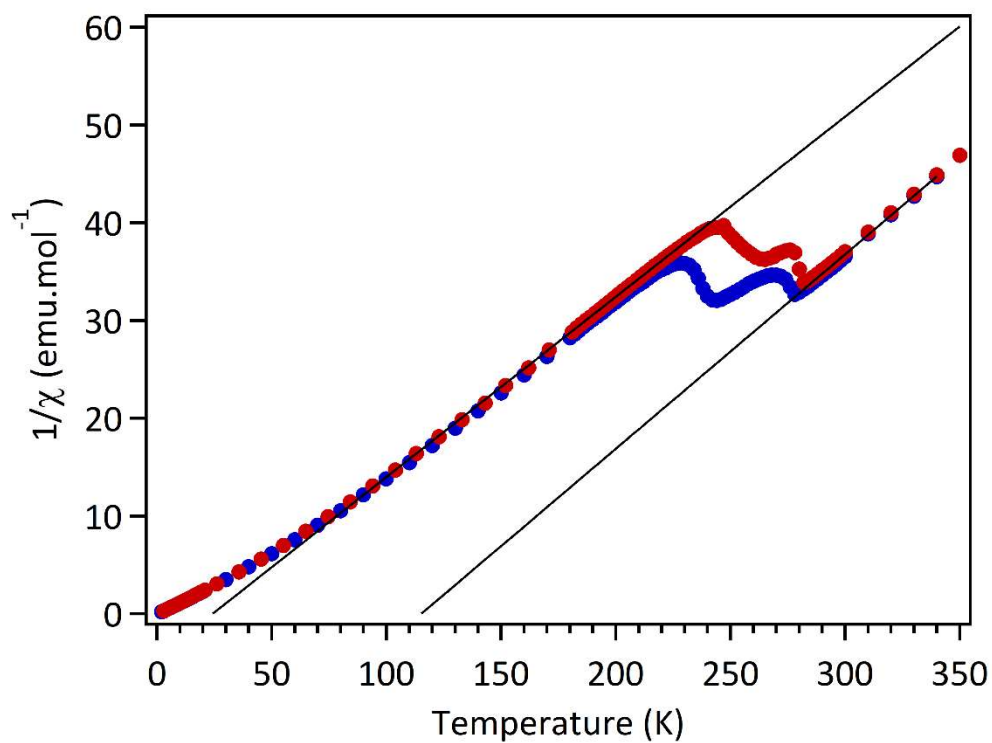
Figure S1. *1/χ vs T* curves of compound **2** while cooling in blue and heating in red. The black curves are the fit for Curie-Weiss regimes.
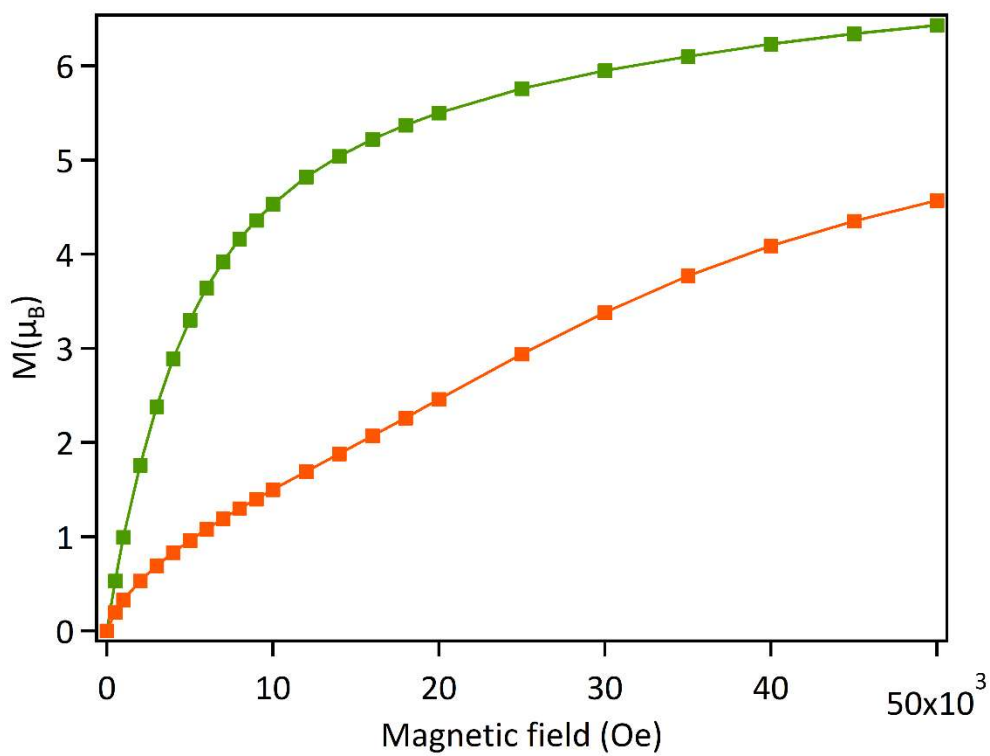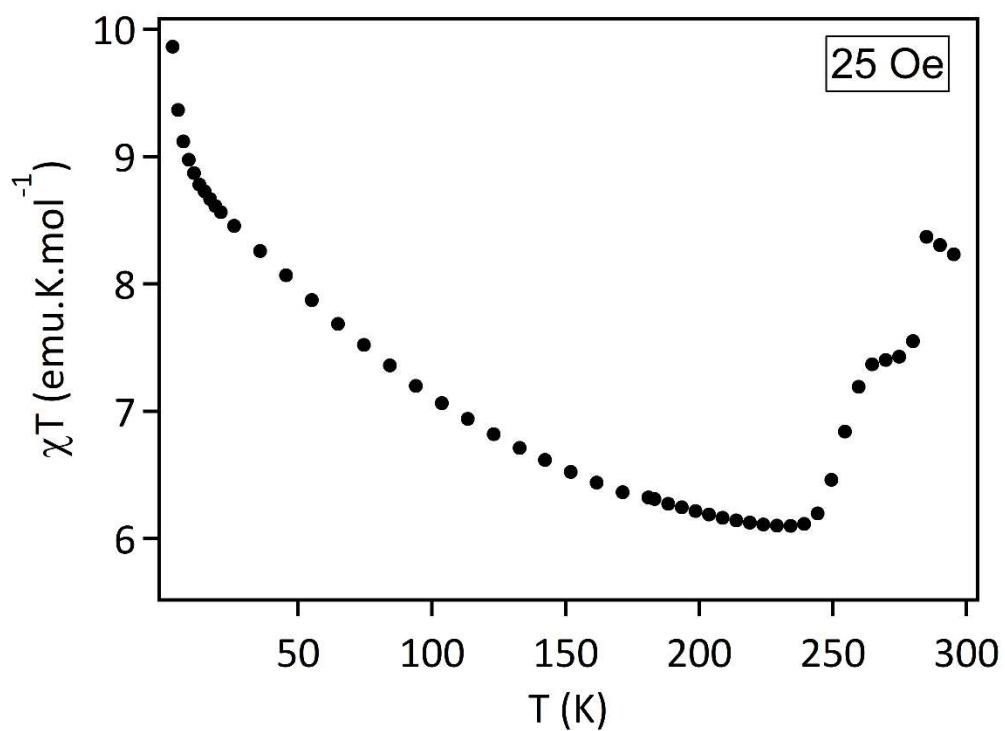

Figure S2. Magnetization curves of compounds **2** (green) and **3** (orange) measured at 2 K in the range of 0-50000 Oe.
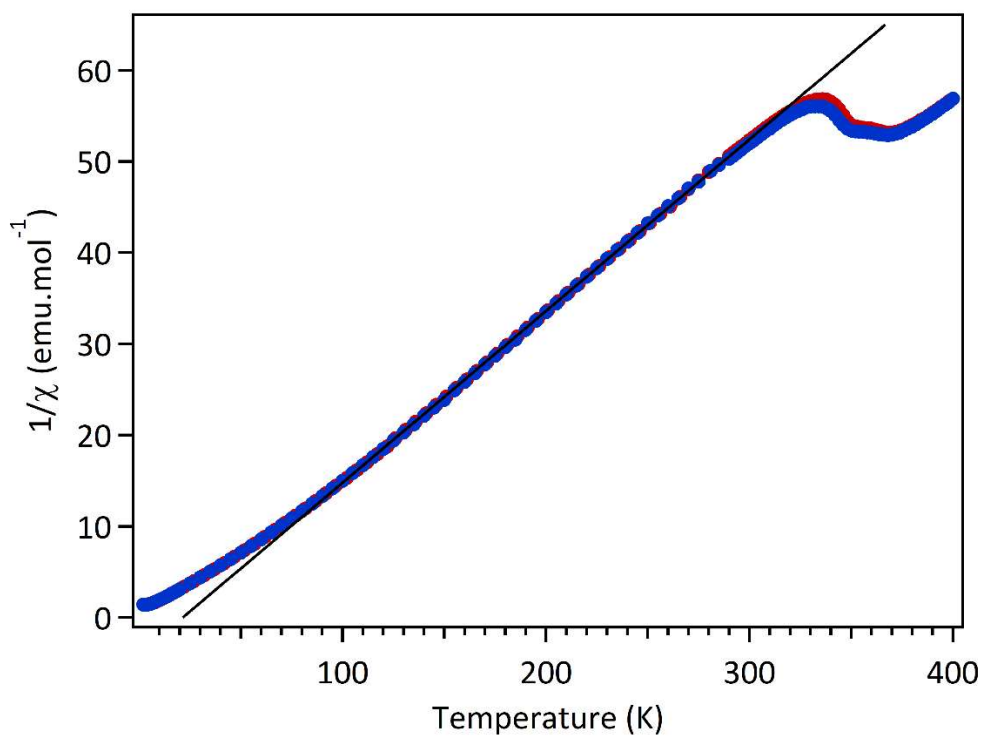
Figure S3. *1/χ vs T* curves of compound **3** while cooling in blue and heating in red. The black curves are the fit for Curie-Weiss regimes.

Figure S4. *χT vs T* curve of compound **2** measured at 25 Oe in heating mode (2-300 K).
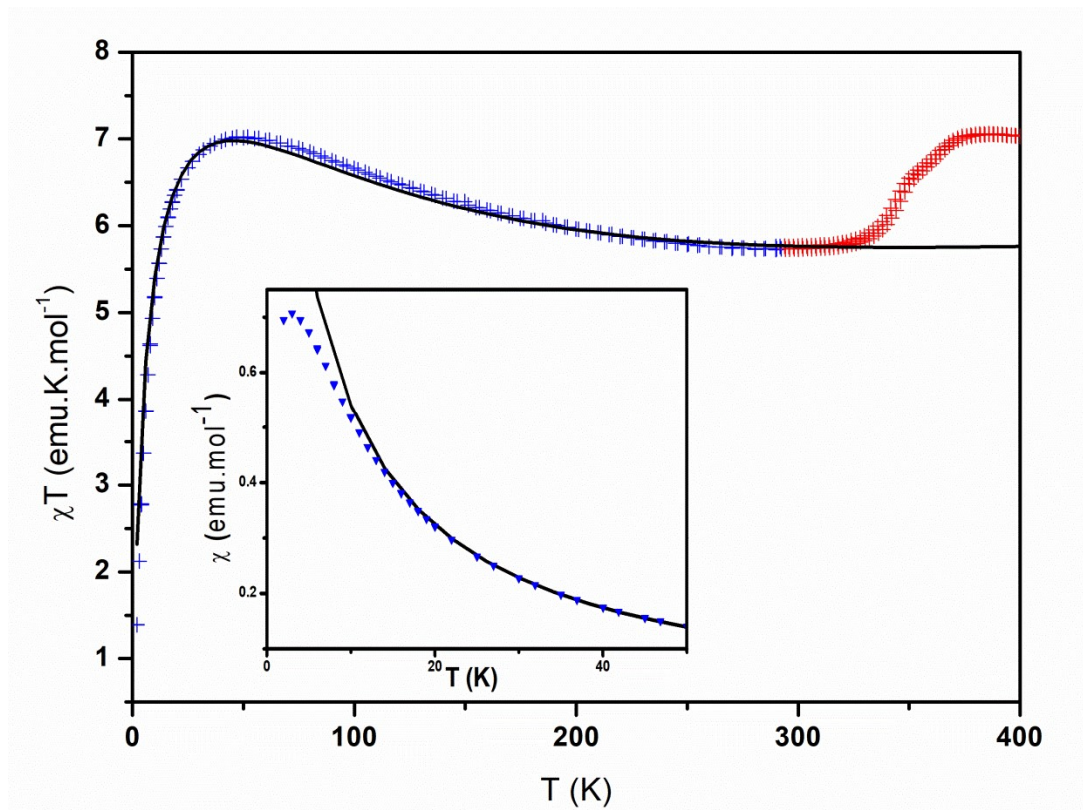
Figure S5. Best fit (solid line) of the low temperature dependence of the χT product (blue cross) for **3** with values in the text $J_{\text{Mn-rad}} = -61(2)$ cm^{-1}, $g_{\text{rad}} = 2$, $g_{\text{Mn}} = 2.04$ and an intermolecular interaction $ZJ = 0.18$ cm^{-1} with $H = 2J(S_{Mn1}S_{rad} + S_{Mn2}S_{rad})$. Inset magnify the maximum in the temperature dependence of magnetic susceptibility (χ) with solid line fit.
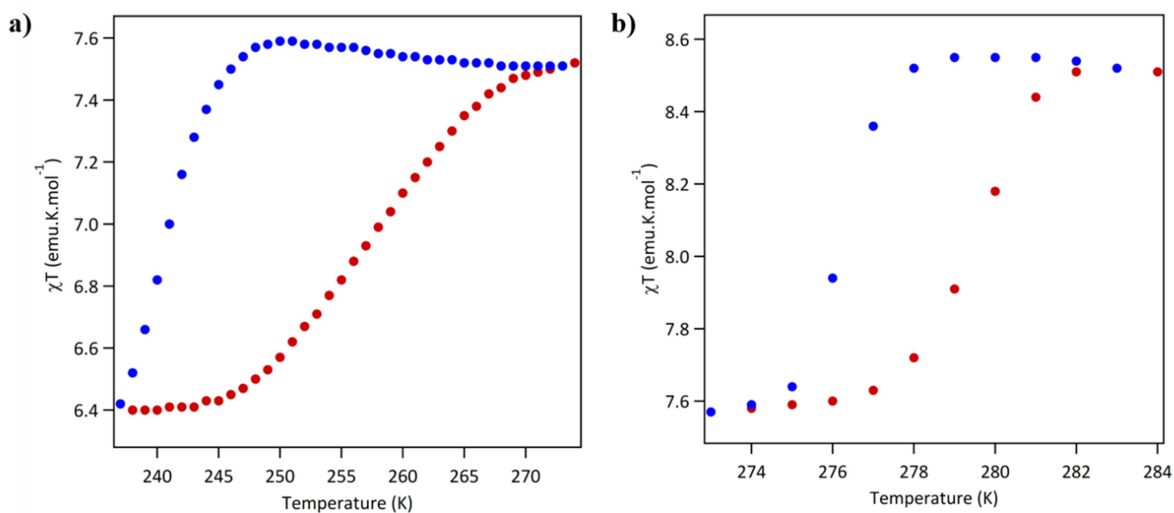
Figure S6. χT vs T curves of compound **2** measured in the temperature range of each hysteresis. a) First step of the VT conversion. b) Second step of the VT conversion.
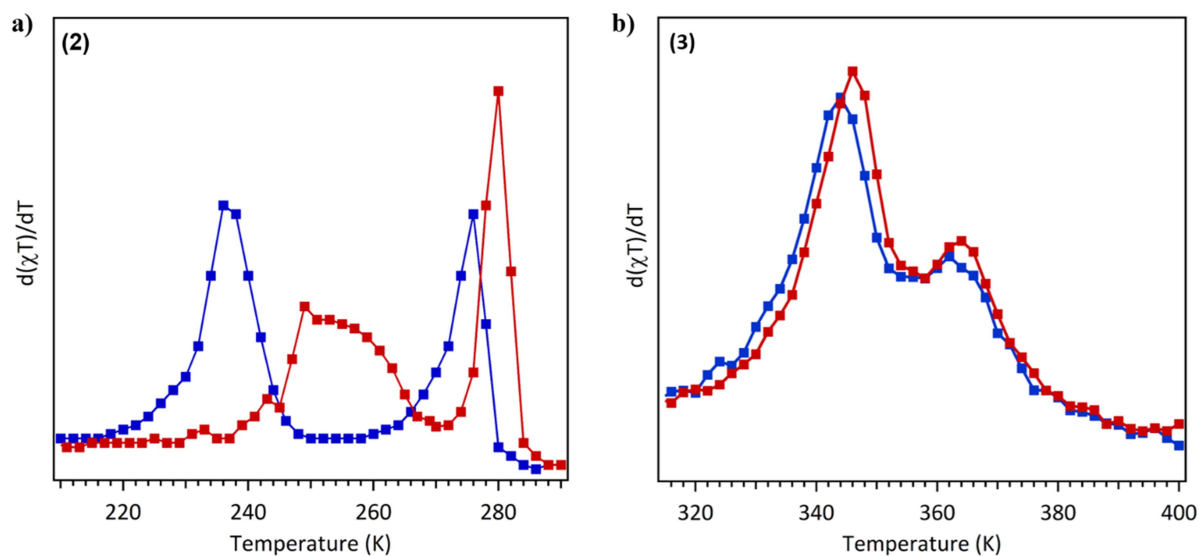
Figure S7. χT derived curves *vs* *T* of compounds **2** (a) and **3** (b). Heating mode in red and cooling mode in blue.
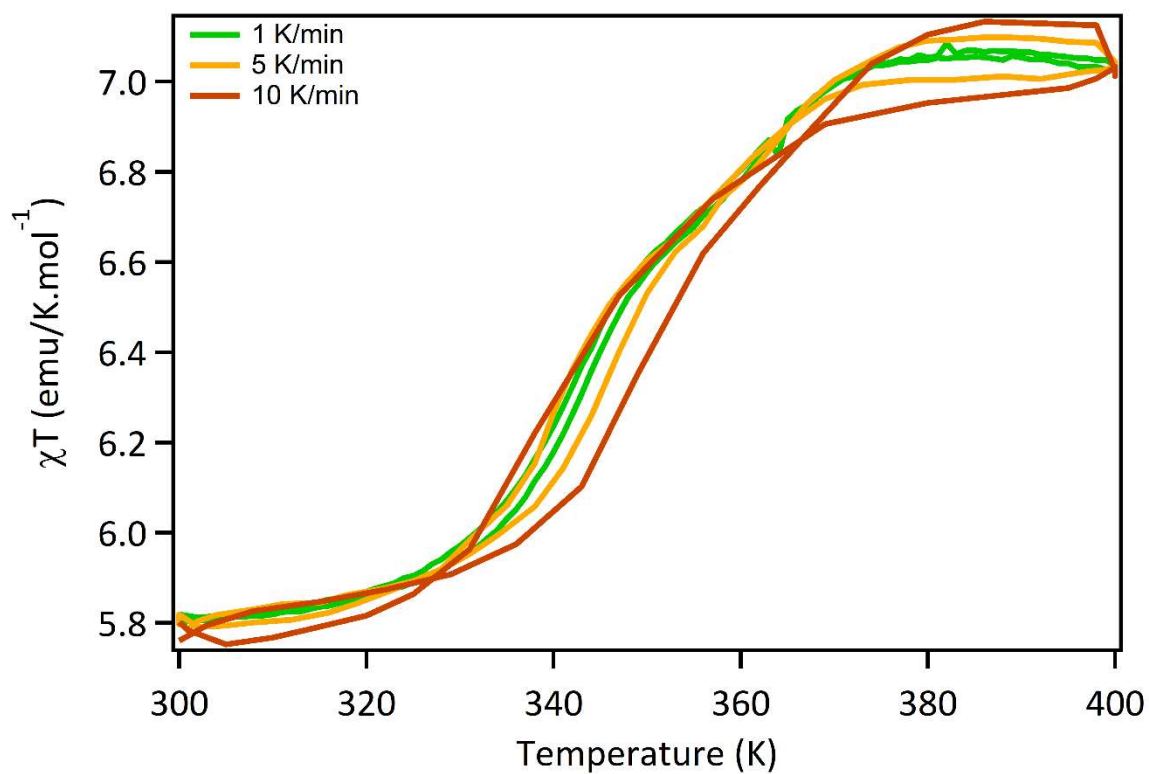
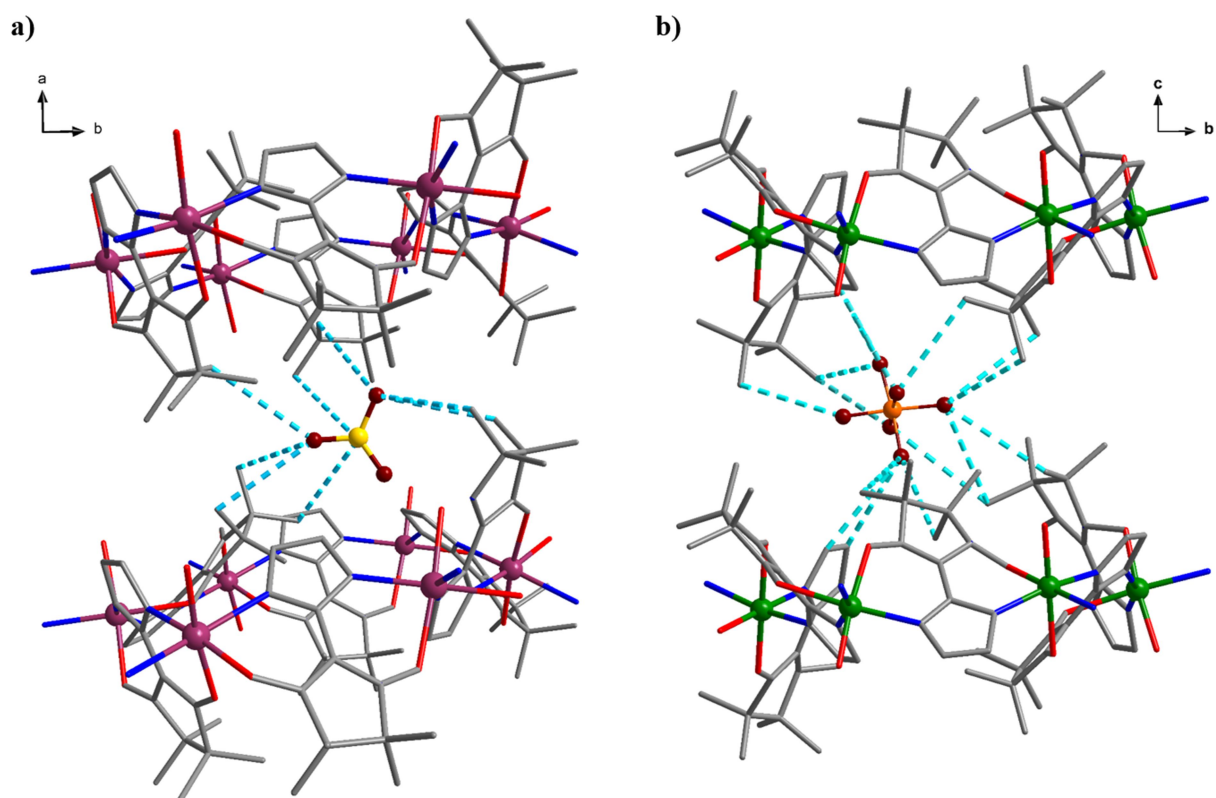**Figure S8.** Scan rate dependence of χT *vs* *T* curves of compound **3**.

Figure S9. Intermolecular contacts depicted in dotted blue lines for **2**$_{HT}$ (a) and **3**$_{LT}$ (b) between the methyl of the radicals and the Fluor of the counter-anion. Only alveoli of two successive sheets along *a*-axis are represented. The atoms are depicted as follows: Mn(II), purple; O, red; N, blue; C, grey; B, yellow; P, orange; F, brown.
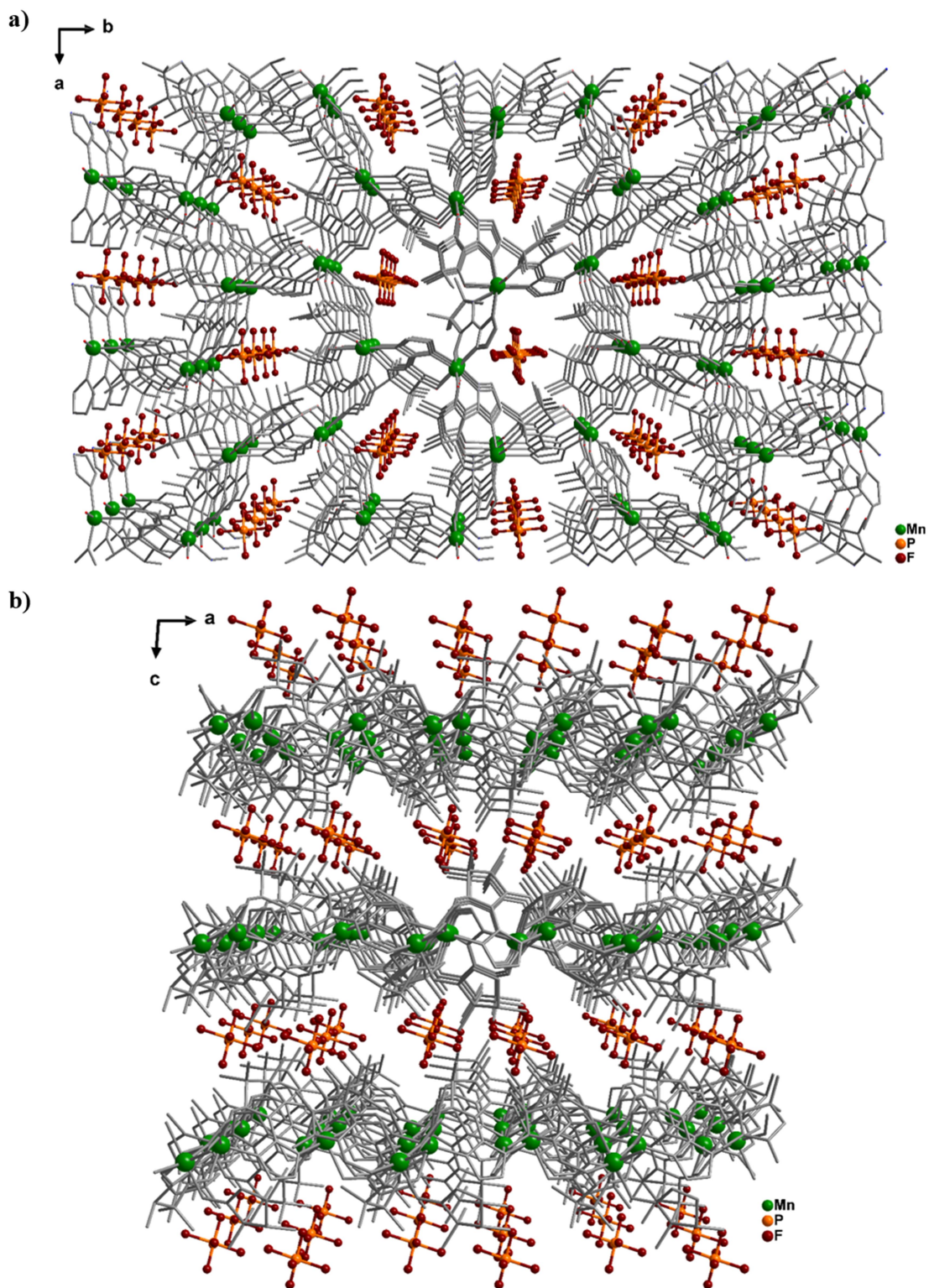
Figure S10. Views of the crystal packing of 3_{LT} phase at 296 K along the *c*-axis (a) magnifying the coordination polymers $\{[Mn^{III}_2(NITIm)(NITRed)_2]\}_n$ and along the *b*-axis (b) showing the intercalated layers of coordination polymers and PF_6^- counter-anions. Atoms are depicted as follows: Mn(III), green; F, brown; P, orange, NITIm⁻, grey.
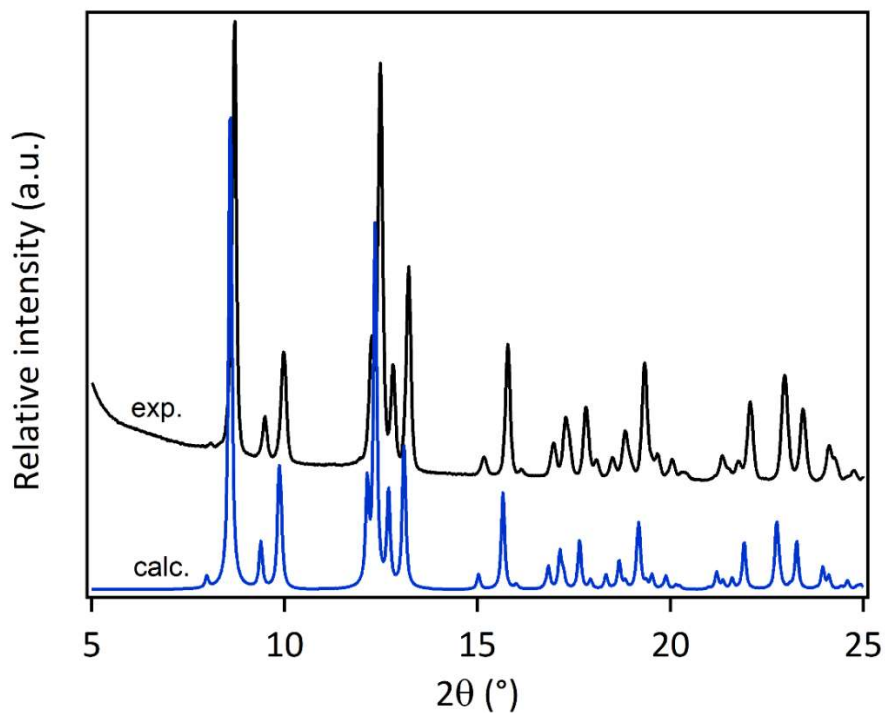
Figure S11. Experimental X-ray powder diffractogram (top: black) of compound **2** together with the calculated one (bottom: blue) from the single crystal structure at 293 K.
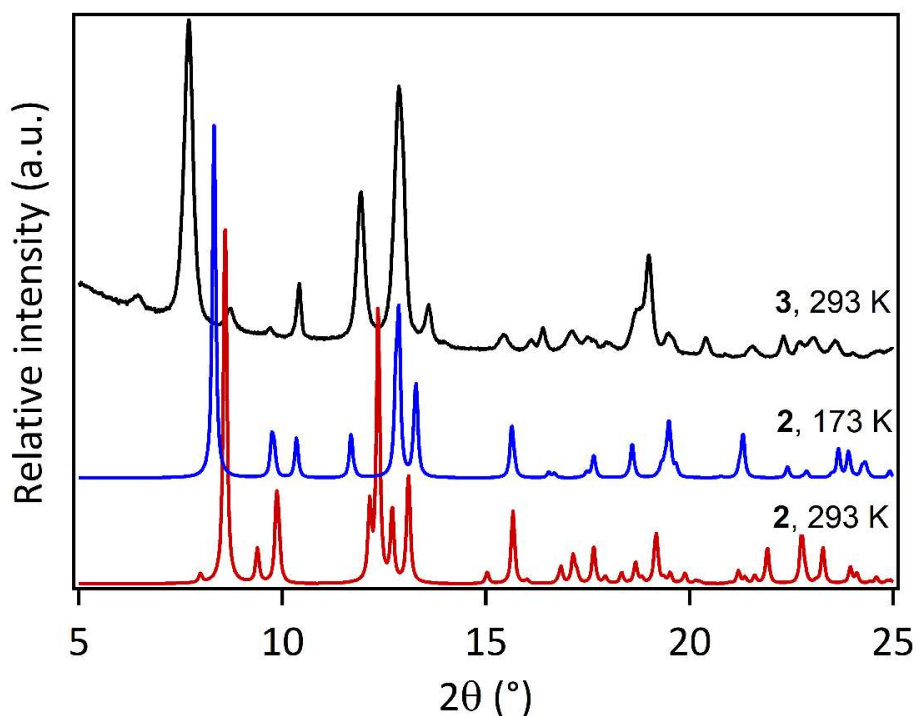

Figure S12. Experimental X-ray powder diffractograms of compound **3** at 293 K (top: black curve) together with the calculated ones from the single crystal structures at 293 K (bottom: red curve) and 173 K (middle blue curve) for compound **2.**
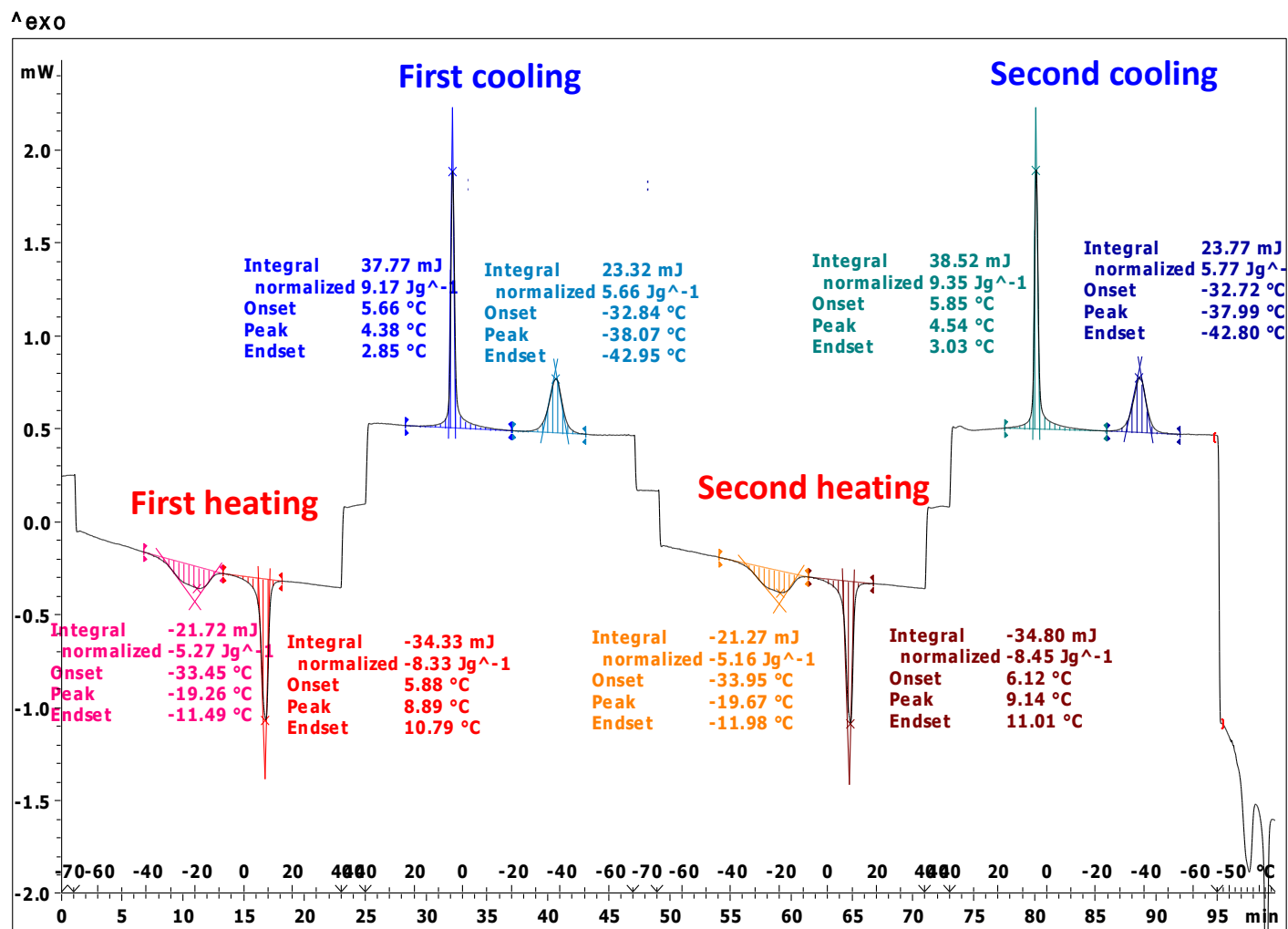
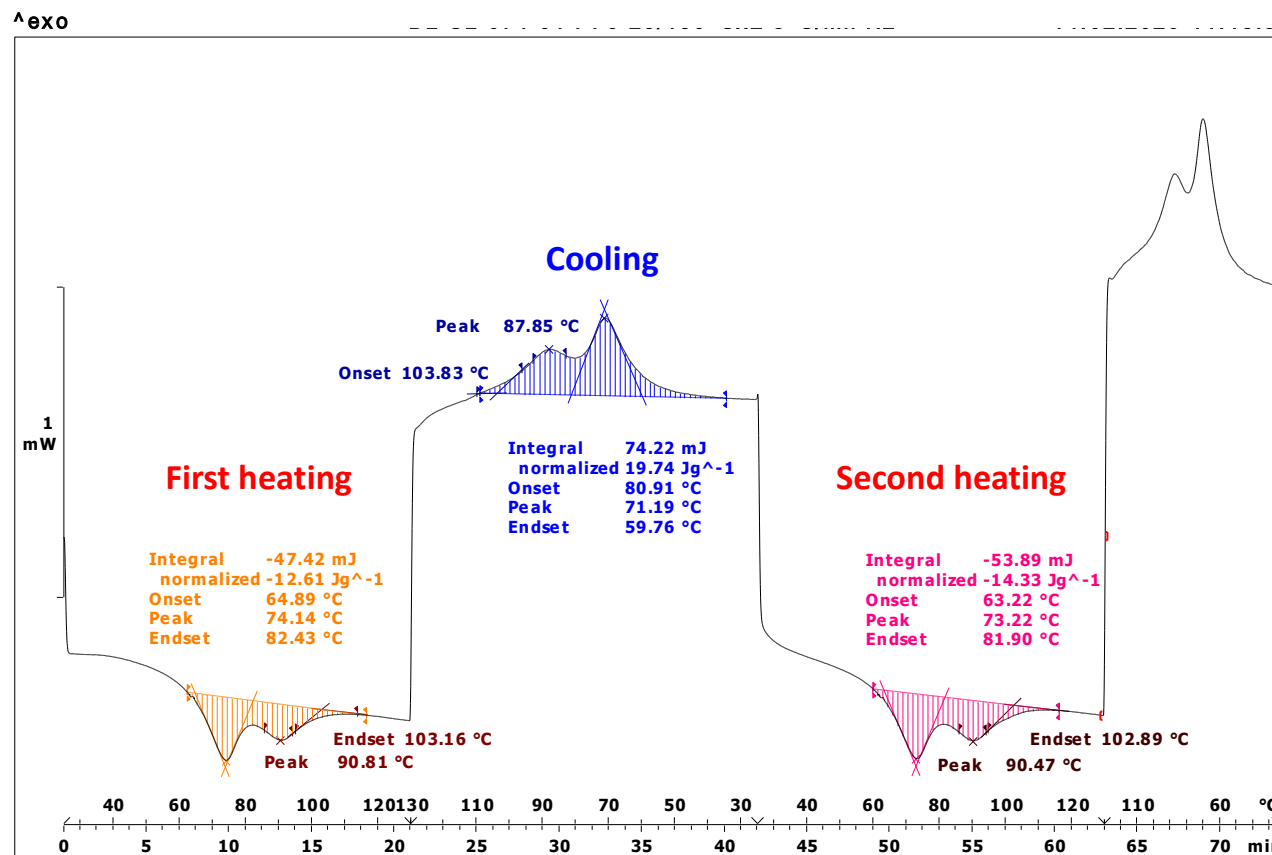**Figure S13**: Differential scanning calorimetry (DSC) for **2** upon heating and cooling at 5 K/min.

Figure S14: Differential scanning calorimetry (DSC) for **3** upon heating and cooling at 5 K/min.
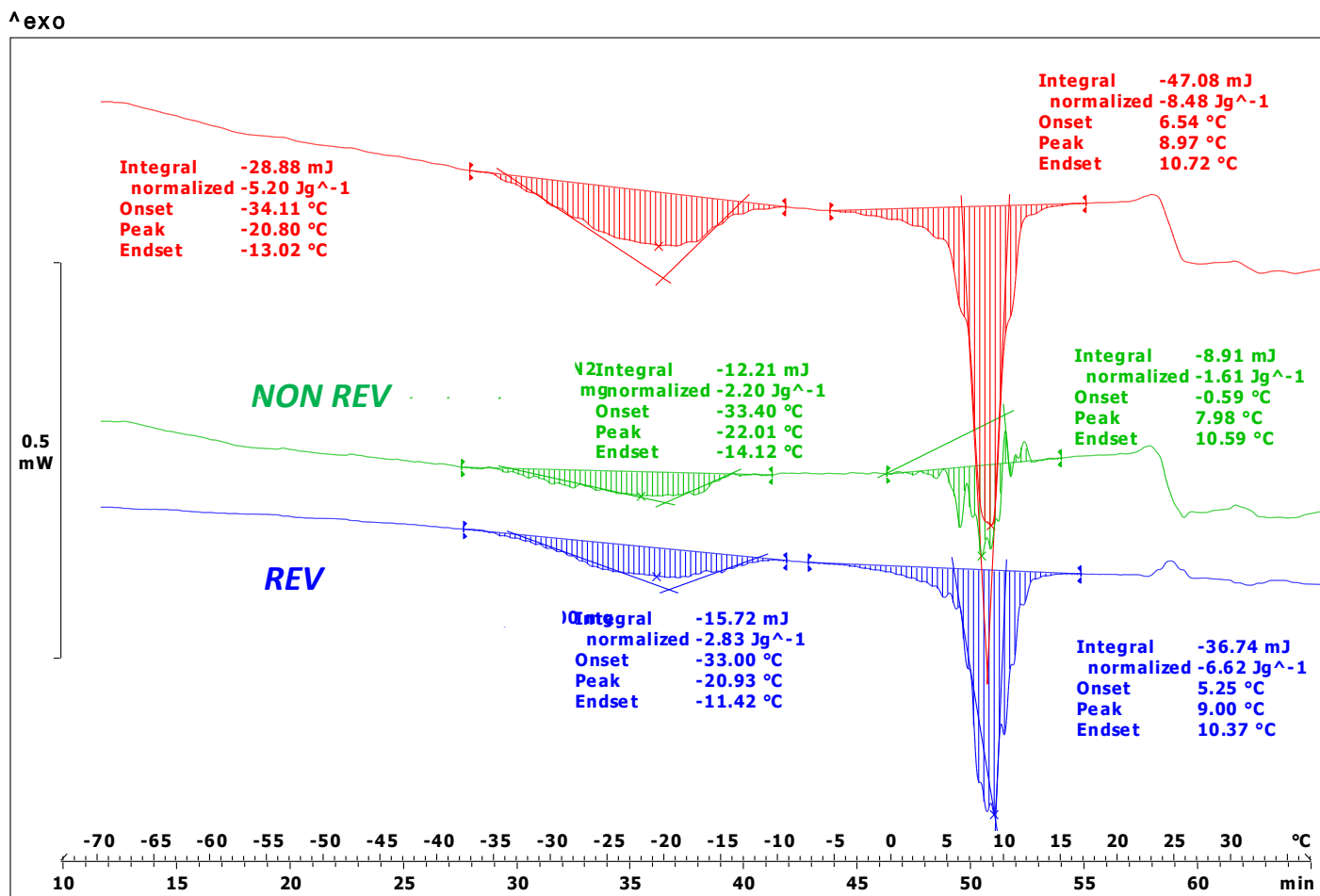
^exo

Integral   -28.88 mJ
 normalized -5.20 Jg^-1
Onset   -34.11 °C
Peak   -20.80 °C
Endset   -13.02 °C

Integral   -47.08 mJ
 normalized -8.48 Jg^-1
Onset   6.54 °C
Peak   8.97 °C
Endset   10.72 °C

NON REV

N2Integral   -12.21 mJ
mgnormalized -2.20 Jg^-1
Onset   -33.40 °C
Peak   -22.01 °C
Endset   -14.12 °C

Integral   -8.91 mJ
 normalized -1.61 Jg^-1
Onset   -0.59 °C
Peak   7.98 °C
Endset   10.59 °C

0.5
mW

REV

Integral   -15.72 mJ
 normalized -2.83 Jg^-1
Onset   -33.00 °C
Peak   -20.93 °C
Endset   -11.42 °C

Integral   -36.74 mJ
 normalized -6.62 Jg^-1
Onset   5.25 °C
Peak   9.00 °C
Endset   10.37 °C

-70 -65 -60 -55 -50 -45 -40 -35 -30 -25 -20 -15 -10 -5   0   5   10   15   20   25   30   °C

10   15   20   25   30   35   40   45   50   55   60   min

Figure S15: Temperature-modulated DSC (MTDSC) measurements for **2** in the heating mode at 2 K/min.
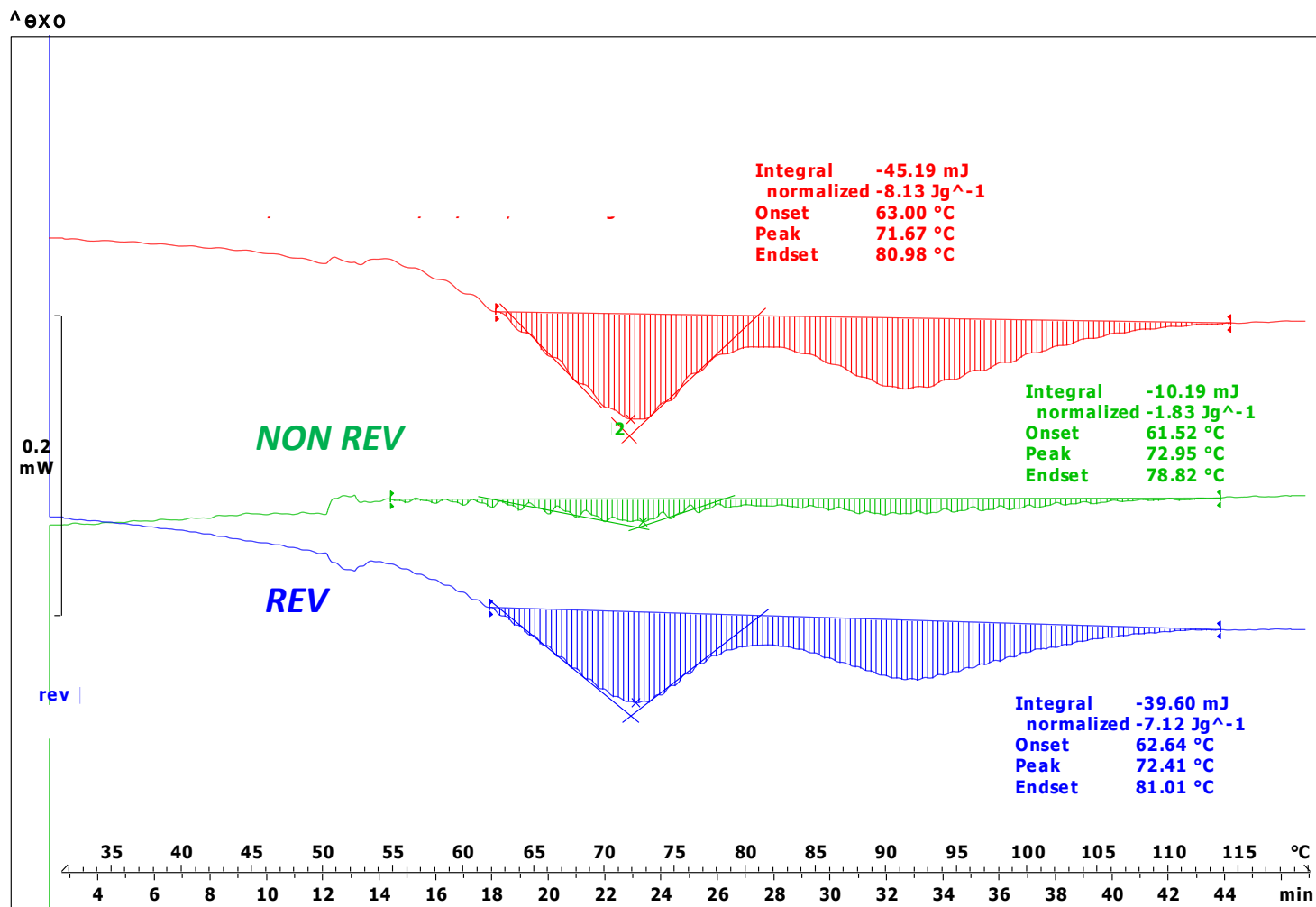
21

Figure S16. Temperature-modulated DSC (MTDSC) measurements for **3** in the heating mode at 2 K/min.
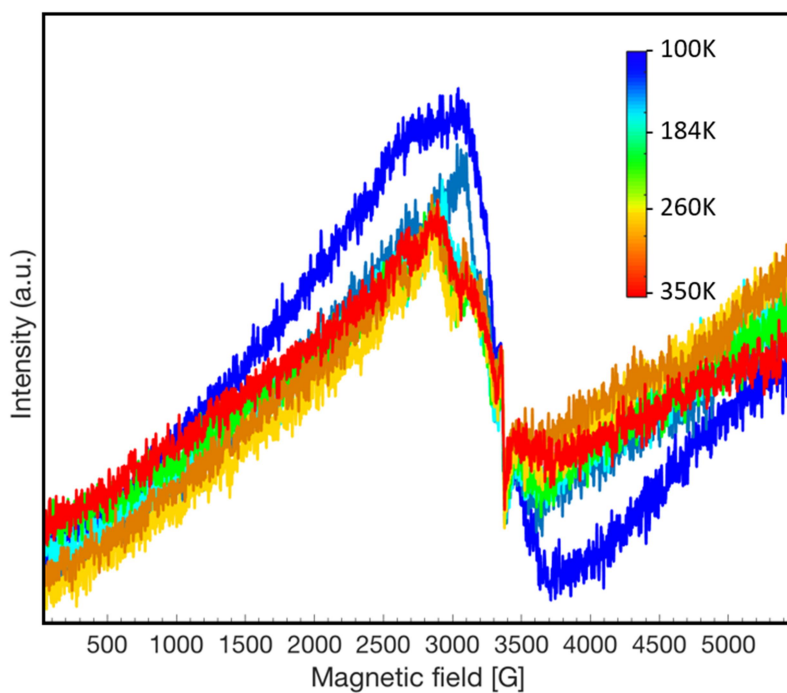
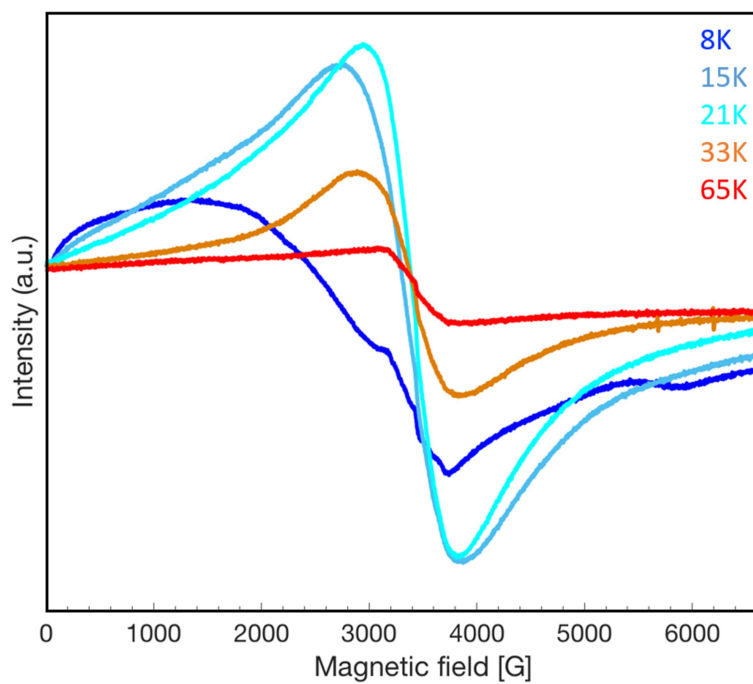**Figure S17.** EPR spectra of compound **3** in perpendicular mode in the temperature range 100-350 K.

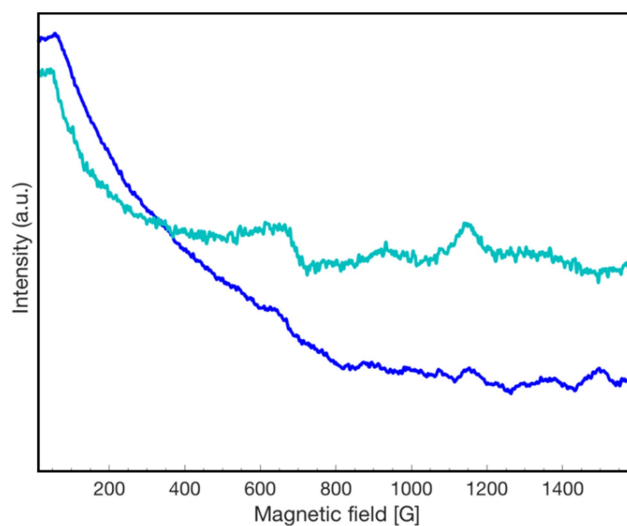**Figure S18.** EPR spectra of compound **3** in perpendicular mode in the temperature range 8-65 K.

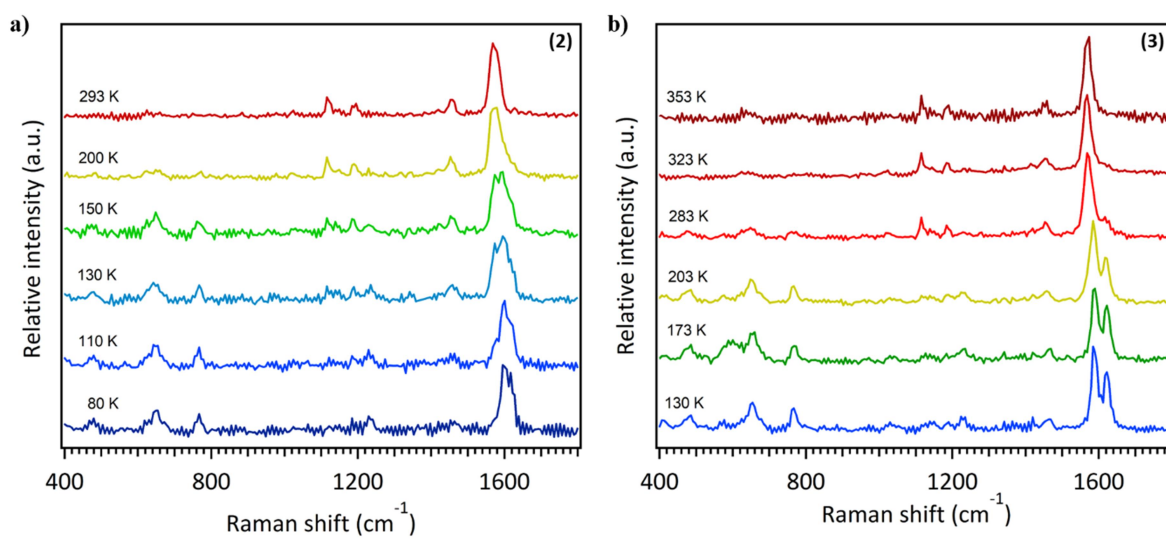**Figure S19**. EPR spectra of compounds **2** (dark blue) and **3** (light blue) at 8 K in parallel mode.

Figure S20. Raman spectra of compound **2** (a) and compound **3** (b) at variable temperature in heating mode.

References:

1. C. Hirel, K. E. Vostrikova, J. Pecaut, V. I. Ovcharenko and P. Rey, *Chem. Eur. J.*, 2001, **7**, 2007-2014.
2. K. Fegy, D. Luneau, T. Ohm, C. Paulsen and P. Rey, *Angew. Chem. Int. Ed.*, 1998, **37**, 1270-1273.
3. Bruker, *Journal*, 2012.
4. Bruker, *Journal*, 2001.
5. A. Lannes, Y. Suffren, J. B. Tommasino, R. Chiriac, F. Toche, L. Khrouz, F. Molton, C. Duboc, I. Kieffer, J. L. Hazemann, C. Reber, A. Hauser and D. Luneau, *J. Am. Chem. Soc.*, 2016, **138**, 16493-16501.
6. Sheldrick G., *Acta Cryst.*, 2015, **C27**, 3-8.
7. L. Farrugia, *J. Appl. Crystallogr.*, 1999, **32**, 837-838.
8. O. V. Dolomanov, L. J. Bourhis, R. J. Gildea, J. A. K. Howard and H. Puschmann, *J. Appl. Crystallogr.*, 2009, **42**, 339-341.
9. L. J. Bourhis, O. V. Dolomanov, R. J. Gildea, J. A. K. Howard and H. Puschmann, *Acta Cryst. A*, 2015, **A71**, 59-71.
10. O. Kahn, *Molecular Magnetism, VCH, New York,*, 1993.
11. P. Pascal, *Ann. Chim. Phys.*, 1910, **19**, 5-70.